Article

Strictosidine Synthase Triggered Enantioselective Synthesis of N-substituted (S)-3,14,18,19-Tetrahydroangustines as novel Topoisomerase I Inhibitors

Yunrui Cai, Huajian Zhu, Zaccary Alperstein, Wenjun Yu, Artem Cherkasov, and Hongbin Zou

ACS Chem. Biol., **Just Accepted Manuscript** • DOI: 10.1021/acschembio.7b00740 • Publication Date (Web): 15 Nov 2017

Just Accepted

ACS Publications

ACS Chemical Biology is published by the American Chemical Society. 1155 Sixteenth Street N.W., Washington, DC 20036

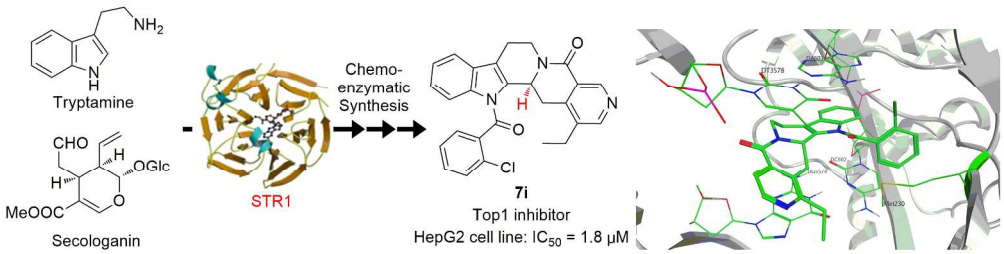

218x54mm (300 x 300 DPI)

Strictosidine Synthase Triggered Enantioselective Synthesis of *N*-substituted (*S*)-3,14,18,19-Tetrahydroangustines as novel Topoisomerase I Inhibitors

Yunrui Cai, [†,‖] Huajian Zhu, [‡,†,‖] Zaccary Alperstein, [§,‖] Wenjun Yu,[†] Artem Cherkasov, [§] Hongbin Zou[†,*]

[†] College of Pharmaceutical Sciences, Zhejiang University, Hangzhou 310058, China

[‡] Zhejiang University City College, Hangzhou 310015, Zhejiang, China

[§] Vancouver Prostate Centre, University of British Columbia, Vancouver, British Columbia V6H 3Z6, Canada

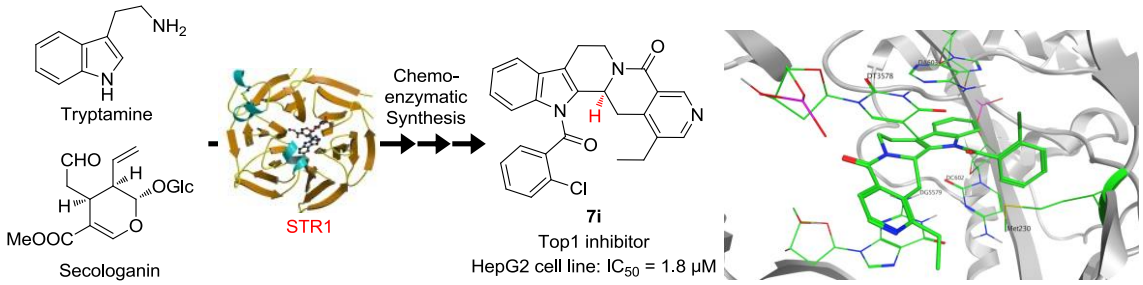

ABSTRACT: Monoterpenoid indole alkaloids (MIAs) comprise an important class of molecules for drug discovery, and these have variant carbon skeletons with prominent bioactivities. For instance, in spite of limitations to their use, camptothecins are the only clinically approved Topoisomerase I (Top1) inhibitors. The enzyme STR1, which is key for MIA biosynthesis, was applied to the enantioselective preparation of three *N*-substituted (*S*)-3,14,18,19-tetrahydroangustine (THA) derivatives. These non-camptothecin MIAs were shown to have moderate *in vitro* HepG2 cytotoxicity and Top1 inhibition activities. The (*S*)-configured MIAs had stronger cytotoxicity and Top1 inhibition than their chemically synthesized (*R*)-enantiomers, which aligned with the results of molecular dynamics simulations. A series of *N*-substituted (*S*)-THAs were then chemo-enzymatically synthesized to investigate structure-activity relationships. The most active analogue observed was the *N*-(2-Cl benzoyl) substituted derivative (**7i**). Insight into the binding mode of **7i** and topoisomerase I-DNA covalent complex was investigated by molecular dynamics simulations, which will facilitate future efforts to optimize the Top1 inhibitory activities of non-camptothecin MIAs.

Monoterpenoid indole alkaloids (MIAs) comprise an important group of natural secondary metabolites [including camptothecin (CPT), ajmaline, vindoline, quinine, and others; Figure 1], and these are famous for their diverse structural skeleton and prominent pharmacological activities.[1,2] Strictosidine synthase (STR1, Figure 1) is a gateway enzyme which conducts asymmetric Pictet-Spengler (P-S) condensation between tryptamine and secologanin to Strictosidine for the biosynthesis of some 2000 MIAs.[3,4] Owing to the critical function of STR1 in the biosynthetic pathway of MIAs, it has been comprehensively studied in chemical biology following the disclosure of its 3D structure.[4–10] The P-S condensation catalyzed by STR1 is very attractive due to its advantages in high stereoselectivity and efficiency as well as mild reaction conditions. However, there are few examples demonstrating the chemo-enzymatic use of STR1 to synthesize new alkaloids in the search for bioactive substances.[5,11] Previously, we reported preparation of several MIAs by one-step syntheses starting from the STR1 reaction product strictosidine.[12]

Since CPT, a natural product MIA[13], was established as a Topoisomerase I (Top1) inhibitor with excellent antitumor activity, Top1 has become a hot-target in cancer chemotherapy due to its role in DNA replication, transcription and other processes through relaxation of supercoiled DNA.[14,15] Although the camptothecins such as Topotecan, Irinotecan and Belotecan were developed as the only three clinically approved Top1 inhibitors,[16,17] they have several limitations to their use specifically including poor chemical stability due to the spontaneous opening of the lactone.[15,17] Therefore, discovery of novel non-CPT Top1 inhibitors has become a promising research field, and several novel Top1 inhibitors have been reported.[18,19] These diversified inhibitors include compounds in clinical trial such as indenoquinolines (BMS-247615, Phase II)[20],

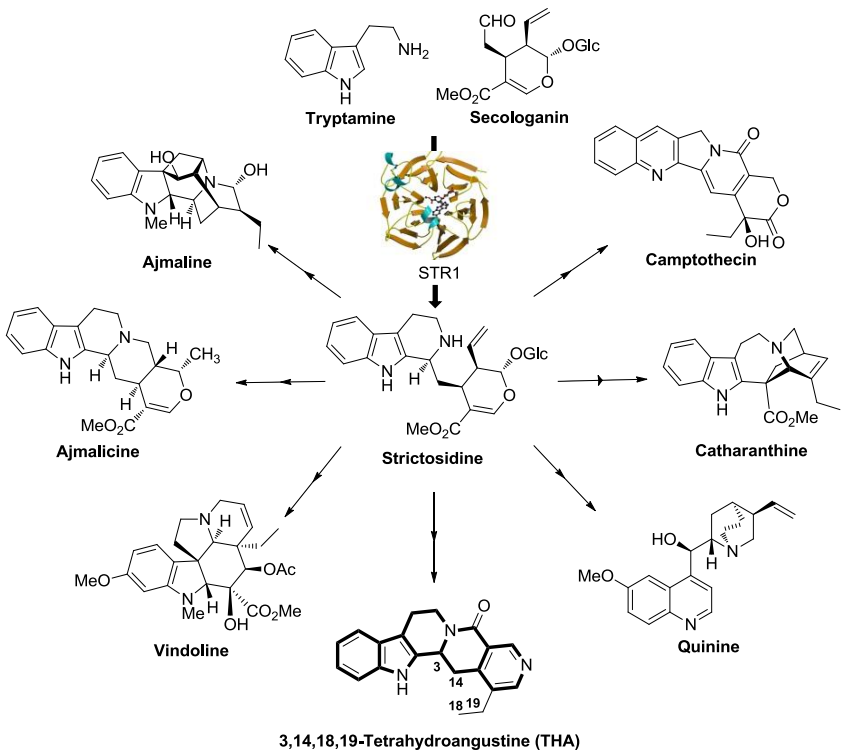

Figure 1. STR1 as gateway enzyme for natural MIAs biosynthesis

indenoisoquinolines (NSC-724998, Phase I)[21], dibenzonaphthyridinones (Genz-644282, Phase I)[22] as well as some molecules under preliminary investigations such as the evodiamines (Figure 2A)[23].

3,14,18,19-Tetrahydroangustine (THA, Figure 1) and angustine are proposed biogenetically as belonging to STR1 catalyzed MIAs, and showed *in vitro* antiproliferative and anti-inflammatory activities.[24,25] When first isolated from *Strychnos angustflpra*[26], the carbon skeleton of angustine aroused significant interest from chemists to attempt total synthesis, and several successful strategies were reported.[27–29] However, these strategies include many steps and low yields, or lack the flexibility for facile analogue production. Notably, the enantiomer 3(*R*)-THA was also generated from

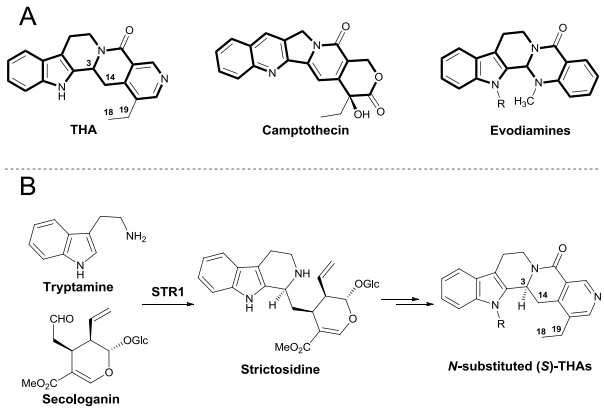

Figure 2. STR1 as biocatalyst for potential Top1 inhibitor THAs

hydrogenated vincosamide, and the selective 3*R* configuration originated from the spontaneously lactamized product of vincoside, isolated from *Adina rubescens*.[30]

Interestingly, the structural arrangement of THA is similar to CPT and the evodiamines (Figure 2A), which suggests that compounds with this skeleton may also be potential Top1 inhibitors. A structure-activity relationship (SAR) study of evodiamines accordingly inspired the synthesis of the *N*-acylated THA derivatives. In order to also identify which configuration might promote the desired bioactivity, 3(*S*)-THAs (**7a**–**c**) were prepared by the STR1 chemoenzymatic approach, and their *R*-enantiomers (**8a**–**c**) were chemically synthesized from vincosamide. Preliminary inhibitory screening results showed that the 3(*S*)-THA derivatives (**7a**–**c**) were superior for both *in vitro* HepG2 cytotoxicity and Top1 inhibition than their (*R*)-enantiomer counterparts (**8a**–**c**), which aligned with the results of molecular dynamics simulations. Initiated by immobilized STR1 as a biocatalyst, a series of 3(*S*)-THAs was stereoselectively generated (Figure 2B) and tested *in vitro* for Top1 inhibitory activity and HepG2 cytotoxicity.

RESULTS AND DISCUSSION

Chemistry. The synthesis of strictosidine can be achieved via the condensation of tryptamine and secologanin in water by reflux in the presence of acetic acid, leading to a mixture of strictosidine and the spontaneously lactamized product of vincoside, vincosamide. Pure vincosamide can be obtained by filtration due to its lower water solubility, leaving a strictosidine mixture that is challenging to purify.[31]

Scheme 1. Synthesis of *N*-substituted THA derivatives[a]

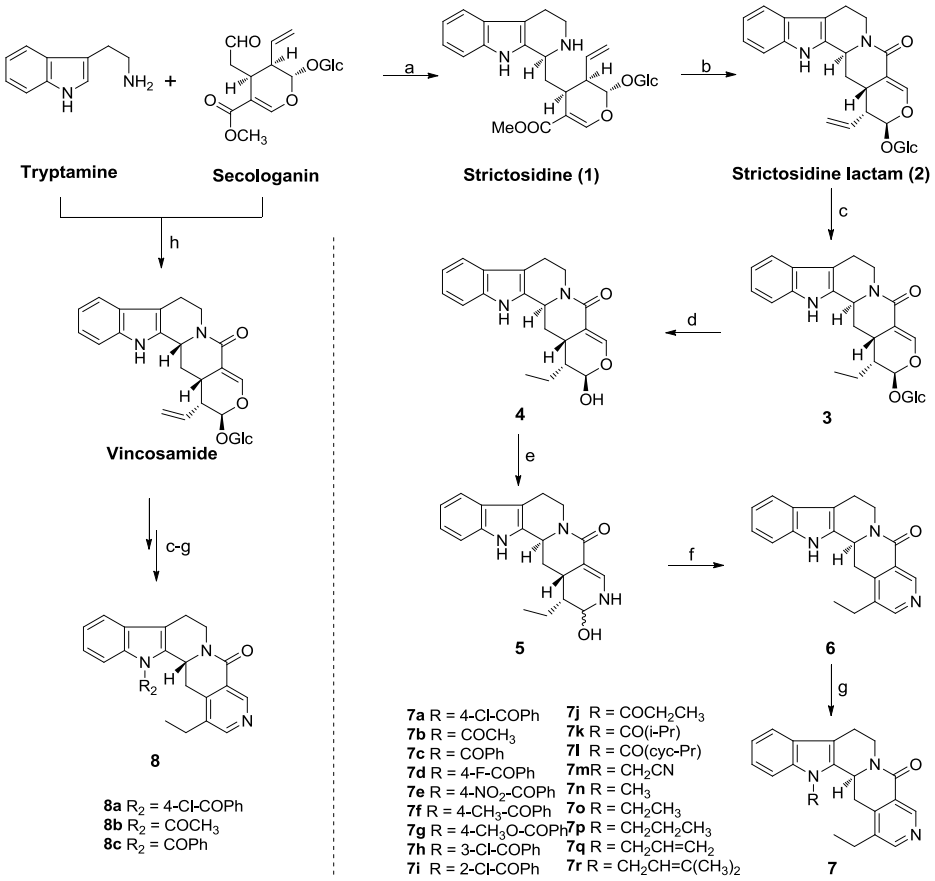

[a] Reagents and conditions: a) STR1, KPi buffer, pH 7.0, 5°C; b) 5% Na_2CO_3, 70 °C; c) H_2, Pd, r.t; d) glucosidase, acetate buffer, pH 5.0, 37 °C; e) NH_4OAc, EtOH, reflux; f) *p*-TsOH, toluene, 90 °C; g) acyl or alkyl halides, *t*-BuOK, THF, r.t.; h) acetic acid, water, reflux

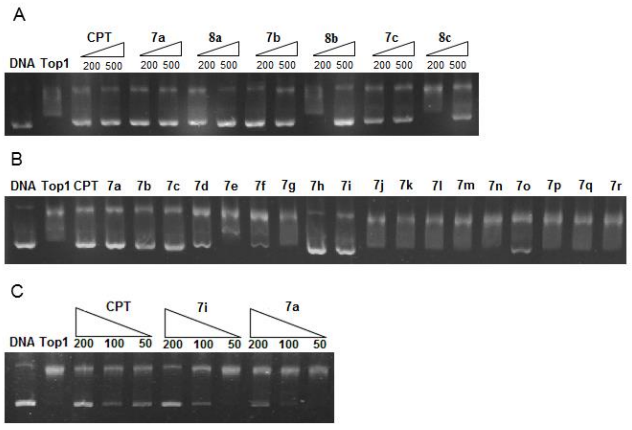

Figure 3. Top1-mediated DNA cleavage assay gel. (A) Inhibition of Top1 relaxation activity at 200 and 500 μM: lane 1, DNA alone; lane 2, DNA + Top1; lane 3–16, DNA + Top1 + CPT or test compounds (**7a**, **8a**, **7b**, **8b**, **7c**, **8c**). (B) Inhibition of Top1 relaxation activity at 200 μM: lane 1, DNA alone; lane 2, DNA + Top1; lanes 3–21, DNA + Top1 + CPT or test compounds (**7a**–**7r**, respectively). (C) Inhibition of Top1 relaxation activity at 50, 100, and 200 μM: lane 1, DNA alone; lane 2, DNA + Top1; lane 3–11, DNA + Top1 + CPT or test compounds (**7a, 7i**).

In the novel approach presented, strictosidine (**1**) was synthesized by the STR1 catalyzed enantioselective P-S reaction of tryptamine and secologanin in mild reaction conditions, and then converted into strictosidine lactam (**2**) in the presence of sodium carbonate. The synthetic routes of *N*-substituted (*S*)-THA derivatives **7a**–**r** and their three *R*-enantiomers **8a**–**c** are depicted in Scheme 1. The hydrogenated product (**3**) of **2** was gently incubated with β-glucosidase, extracted from almonds, to give its aglycone (**4**), which reacted with ammonium acetate in refluxing ethanol to afford its E ring aza- product (**5**). Reaction of compound **5** with *p*-toluenesulfonic acid (*p*-TsOH) in refluxing toluene led to dehydration and oxidation to provide the hetero-aromatized (*S*)-THA (**6**). In the presence of potassium *tert*-butoxide (*t*-BuOK), compound **6** was treated with acyl or alkyl halides to give the *N*-substituted (*S*)-THA derivatives **7a**–**r**. With vincosamide in hand, the same strategy was applied to prepare the corresponding *N*-substituted (*R*)-3,14,18,19-THA derivatives (**8a**–**c**).

The study of the favorable configuration of C-3. In order to identify the favorable configuration of C-3, six *N*-substituted THA derivatives (**7a**–**c**, **8a**–**c**) were synthesized and screened for *in vitro* Top1 inhibitory activity and

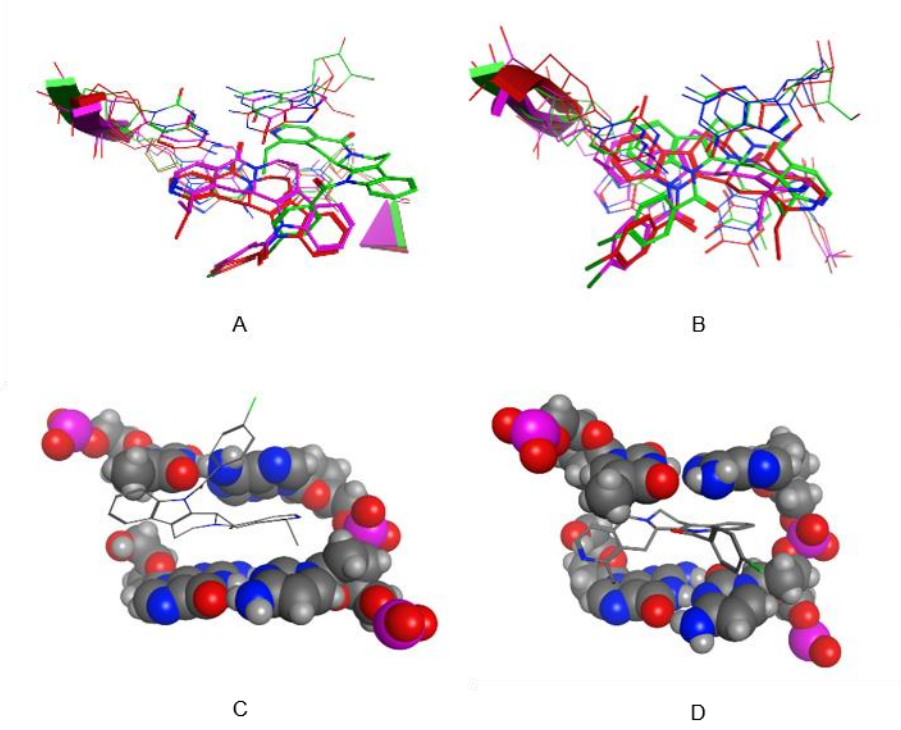

Figure 4. Molecular dynamics (MD) simulations of **7a** and **8a** in Top1 (PDB ID: 1k4t). . (A) Three evenly spaced snapshots taken from the simulations of **8a** in the color-coded order of Green, red, and purple. (B) Three evenly spaced snapshots taken of the simulation with compound **7a**, in the color-coded order of Green, red, and purple. (C) Final snapshot of the simulations of **8a**. (D) Final snapshot of the simulation of **7a.** In all of the picture the protein and most of the DNA has been removed for clarity.

Table 1. *In vitro* cytotoxic activity of the THAs enantiomers against HepG2

Compound	Cytotoxicity (IC_{50}, μM)	Compound	Cytotoxicity (IC_{50}, μM)
7a	8.5 ±0.06	**8a**	29.2 ±0.19
7b	20.9 ±0.09	**8b**	65.2 ±0.24
7c	23.4 ±0.17	**8c**	57.8 ±0.11
CPT	0.68 ±0.01		

antiproliferative activity using HepG2 cells**.** Many Top1 inhibitors act by stabilizing a covalent Top1-DNA, so-called "cleavable complex", to prevent the relaxation of supercoiled DNA. To investigate the inhibitory activity, Top1 and supercoiled DNA pBR322 were incubated in the presence of the test compounds or CPT. Inhibition was observed when the supercoiled complexes were prevented from being relaxed. As shown in Figure 3A, compounds **7a**–**c** and **8a**–**c** are all active against Top1-mediated relaxation of supercoiled DNA at a high concentration (500 μM), indicating that *N*-substituted THA derivatives were novel non-CPT inhibitors of Top1. At lower concentration (200 μM), **7a**–**c** and **8a** maintained inhibition, while none was observed for **8b** and **8c**. Meanwhile, compound **7a** is slightly more preventive of supercoiled DNA relaxation than its enantiomer (**8a)**. These results suggest that *N*-substituted THA derivatives with the *S* configuration possess better Top1 inhibitory activities than their *R*-enantiomers.

To further test the hypothesis of preferred C-3 configuration, compounds **7a**–**c** and **8a**–**c** were also assayed for their *in vitro* cytotoxic activities against HepG2 cell line using the MTT assay. The results listed in Table 1 also showed that *N*-substituted THA derivatives with *S* configuration (**7a**–**c**) are each about three-fold more potent than their *R*-enantiomers. In addition, compound **7a**, having a 4-chlorobenzoyl substituent, exhibited the most potent cytotoxic activity of the analogues tested, which was consistent with the observed Top1 inhibitory activity.

In order to rationalize the differences between the *S*- and *R*- enantiomers of the parent compounds (**7a**–**c** and **8a**–**c**), molecular dynamics (MD) simulations were performed with the OPLS3 force field implemented in Maestro 2016-3 software (Figure 4).[32-37] The docked structures of the *S*-enantiomer (**7a)** and *R*-enantiomer (**8a)** in topoisomerase I (pdb: 1k4t) were simulated for 156 ns and 100 ns, respectively, and visualized with the MOE suite software. After the first ~60 ns of the simulation of compound **8a**, most of the compound was observed to be pushed out of the DNA

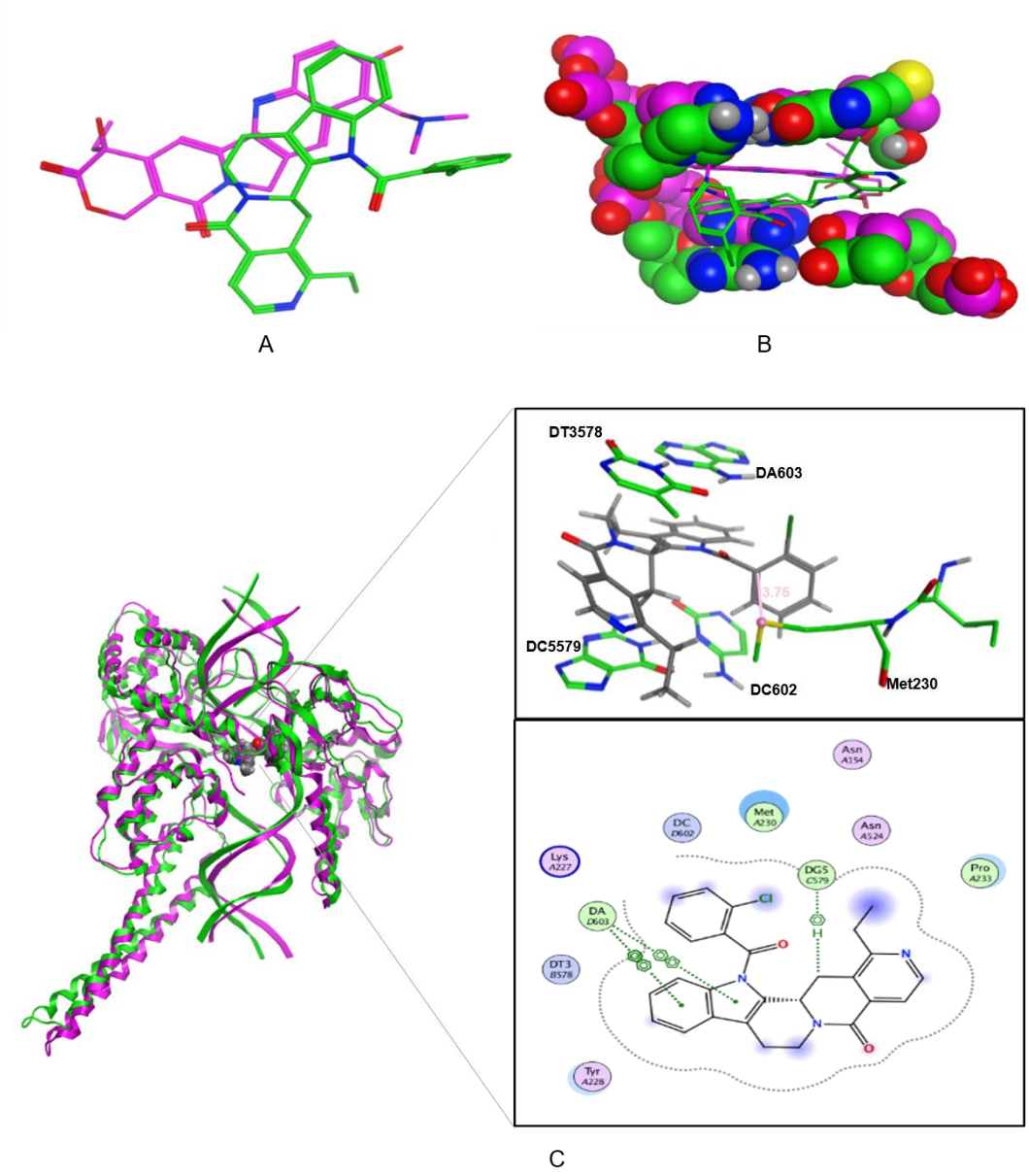

Figure 5. (A) Superimposed docked complexes of **7i** (green) and CPT (purple). (B) Comparison of the final snapshot of **7i** (green) with CPT (purple) in Top1-DNA complex. (C) Binding mode of compounds **7i** and 3D superimposed structure of the final simulated snapshot (gray). In the PDB entry 14kt, Met 230 and Lys 334 correspond to Met 428, and Lys 751.

leaving only part of the pyridine ring left between the bases. The system was simulated for another 100 ns to see if the compound would find its way back between the nucleobases. This was not observed, however, after a 100 ns simulation of compound **7a**, an induced fit was observed with pi-stacking interactions that remained strong throughout the simulation (Figure 4B). To accommodate compound **7a**, the pocket between the DNA increased vertically by around 1 Angstrom (Figure 5B, green). Furthermore, it can be seen that adding large substituents on the *R* enantiomer results in an even more unfavorable geometry, due to the steric interaction resulting from the large out of plane angle of the stereocenter (Figure 4C). Therefore, it appears that the lack of potency of this set in the *R*-enantiomers was largely correlated to the out of plane between the indole ring and the rest of the ring system. The *S*-enantiomer is much more planar, facing more empty room in the pocket, allowing for free substitution on the indole nitrogen (Figure 4D. This explains the greater flexibility in modifications permitted to the *S*-enantiomer, with the 4-chlorobenzoyl analogue having exhibited the most potent cytotoxic activity of the compounds tested.

Structure-activity relationship study. Substituted benzoyl, acyl, cyano, and alkyl groups were introduced to

prepare *N*-substituted (*S*)-THA derivatives **7d**–**r** for SAR study (Scheme 1). As shown in Figure 3B, at the concentration of 200 μM, compounds **7a**–**c**, **7h**, **7i** were found to be active against Top1-mediated relaxation of supercoiled DNA, while compounds **7d**, **7f**, **7o** showed moderate Top1 inhibitory activity, and the rest were almost inactive. Overall, *N*-benzoyl compounds exhibited the most potent Top1 inhibitory activity, especially those with the Cl-substituted benzoyl group (**7a**, **7h**–**i**). This can be understood by the results of the simulation, where it is apparent that the benzoyl ring makes a close interaction with a methionine residue from Top1 (Figure 5C). Compound **7i** was then selected to test the *in vitro* Top1 inhibitory activity at three different concentrations with **7a** and CPT as control (Figure 3C). Furthermore, the antiproliferative activity of **7a**–**r** against HepG2 cell lines was investigated using CPT as a reference drug. As shown in Table 2, compound **7i** was the most potent *in vitro* antiproliferative agent against HepG2, with an IC_{50} value of 1.8 μM. Overall, IC_{50} values of most *N*-benzoyl compounds and some *N*-acylated compounds were < 10 μM, but most *N*-alkylated compounds exhibited weak cytotoxicity. Taken together, the results of cytotoxicity assay are consistent with Top1 inhibitory activity.

Table 2. Antiproliferative activity of the *N*-Substituted (*S*)-THA derivatives against HepG2

Compound	Cytotoxicity (IC_{50}, μM)	Compound	Cytotoxicity (IC_{50}, μM)
7a	9.1 ±0.02	**7k**	18.2 ±0.03
7b	16.6 ±0.08	**7l**	9.6 ±0.02
7c	23.5 ±0.09	**7m**	24.6 ±0.15
7d	7.5 ±0.01	**7n**	na[a]
7e	9,7 ±0.03	**7o**	33.5 ±0.24
7f	5.6 ±0.01	**7p**	na[a]
7g	8.3 ±0.02	**7q**	na[a]
7h	12.3 ±0.02	**7r**	na[a]
7i	1.8 ±0.01	CPT	0.70 ±0.004
7j	5.2 ±0.03		

[a] na= not active

To further understand the contribution toward Top1 inhibition of the novel THA pharmacophore, the most active derivative, compound **7i**, was compared with CPT by docking into the final snapshot of the 7a simulated structure, and superimposing this with the CPT crystal structure (Figure 5). The overlap of A, B, and C rings between these molecules suggested their similar binding modes (Figure 5A). Interestingly, both internal amides of the two compounds overlapped in their nitrogen and carbonyl oxygen atoms in the same region, perhaps satisfying an electrostatic need. In addition, compound **7i** was observed to induce its fit into the cleaved DNA complex with topoisomerase I by increasing the size of the gap between the DNA bases relative to CPT (Figure 5B), in which **7i** is stabilized by additional amino acid contacts that predominantly include methionine. This interaction appears to be driven by a strong aromatic-dipole interaction at the *ortho*-substituted benzoyl ring with methionine 428 (Figure 5C). Interestingly, during the simulation of compound **7a** a strong water mediated contact with lysine 751 of Top1 was observed for more than half of the simulation (Supplementary Figure S1, S2).

Conclusion. In summary, immobilized STR1 was utilized to enantioselectively synthesize a series of *N*-substituted (*S*)-THA derivatives and successfully provide a short and efficient chemo-enzymatic approach to prepare polycyclic MIAs. These *N*-substituted (*S*)-THAs were identified as novel Top1 inhibitors. Interestingly, the Top1 and HepG2 inhibitory activities observed *in vitro* showed that the C-3(*S*) configuration of *N*-substituted THAs are preferred for bioactivity. This was supported by MD simulation models that the *R*-enantiomer may be pushed out of pocket of Top1 while the corresponding *S*-enantiomer may remain between the bases. Moreover, the SAR study of *N*-substituted (*S*)-THAs was conducted, and the Top1 inhibitor **7i** was identified as the most potent analogue tested. The formation a novel methionine-aromatic contact between **7i** and Top1 was proposed to explain the observed activity. Indeed, this type of strong interaction is only beginning to be recognized as a stabilizing force in protein structures.[38] The results described here provide further insight into the biocatalytic character of STR1, and demonstrate an excellent opportunity for its use as a biocatalyst for the enantioselective construction of diversified MIAs with potentially meaningful bioactivity.

METHODS

Materials. Secologanin was isolated from *Lonicera Tatarica*. Topoisomerase I, purified from calf thymus was purchased from Thermo Fisher Scientific. All of the other chemicals were obtained from commercial sources.

Synthesis of *N*-substituted THAs. Synthetic methods are summarized in the legends of Schemes 1. Fully detailed protocols, along with the characterization of synthetic products by NMR and MS, are described in detail in the Supporting Information.

Topoisomerase I Inhibition Assay. The enzyme activity was measured by assessing relaxation of supercoiled pBR322 plasmid DNA. Test compounds were dissolved in DMSO and were tested at final concentrations as shown. The reaction mixture contained 2 × DNA Top1 buffer (10 μL), Top1 (0.5 U), the test compounds (various concentrations), pBR322 plasmid DNA (0.25 μg), and distilled water in a final volume of 20 μL. Reactions were carried out for 30 min at 37 ℃ and then stopped by adding SDS [0.5% (w/v) final concentration]. After that, 3.5 μL of 6 × loading buffer [0.1 mM EDTA, 7% (v/v) glycerol, 0.01% (w/v) xylene cyanol FF, 0.01% (w/v) bromophenol blue] was added.

Reaction products were electrophoresed on a 0.8% (w/v) agarose gel in TAE (Tris-acetate-EDTA) running buffer at 60 V for 1.5 h. To visualize the reaction products, the gel was stained with 0.5 μg mL^{-1} ethidium bromide for 10 min. DNA bands were visualized using a UV transilluminator.

***In Vitro* Cytotoxicity Assay.** Cells were plated in 96-well microtiter plates at a density of 5×10^3 cells/well and incubated in a humidified atmosphere with 5% CO_2 at 37 ℃ for 24 h. Test compounds were added to wells at different concentrations, and 0.1% (v/v) DMSO was used as a control. After samples were incubated for 72 h, 20 μL of MTT (3-(4,5-dimethylthiazol-2-yl)-2,5-diphenyl-tetrazolium-bromide) solution (5 mg mL^{-1}) was added to each well, and the plate was incubated for an additional 4 h. The formazan was dissolved in 100 μL of DMSO. The absorbance (OD) was quantitated with microplate spectrophotometer at 570 nm. Wells containing no drugs were used as blanks for the spectrophotometer. The survival of the cells was expressed as percentage of untreated control wells. All experiments were performed in triplicate.

Molecular Docking. The 1k4t entry of topoisomerase I downloaded from the protein data bank, and prepared with the Schrodinger Maestro protein preparation software module.[32] Briefly, all original hydrogens were removed and re-added, crystallographic ions and waters were removed, and the propka optimizer at pH 7.4 was used to calculate the amino acid protonation states. The structure was then minimized with CPT using the OPLS3 force field. Furthermore, the crystal structure was used to dock THA derivatives with the Glide module on XP mode, and used as a starting point for the simulation[33–35]. The highest scored structure were used to prepare the simulated systems.

Molecular Dynamics Simulations. The MD simulation was done with the Desmond molecular dynamics engine with OPLS3. Explicit solvent was used with the SPC water model and 0.15 M NaCl to mimic physiological conditions. The NPT ensemble was used at a constant temperature and pressure of 300 K and 1.01 bar with the Nose-Hoover chain thermostat, and the Martyna-Tobias-Klein isotropic barostat.[36,37] The pictures were rendered and taken with the MOE software suite. Analysis was done with the Schrodinger simulation interactions script.

AUTHOR INFORMATION

Corresponding Author

*E-mail: zouhb@zju.edu.cn

Author Contributions

‖These authors contributed equally to this work.

Notes

The authors declare no competing financial interest.

THA in this paper is the abbreviation of 3,14,18,19-Tetrahydroangustine.

ACKNOWLEDGMENTS

This work was supported by the National Natural Science Foundation of China (No. 21472170, 21272207, 21702183), the Zhejiang Provincial Fund for Distinguished Young Scholars (LR15B020001), the National High-tech Research and Development Program (863 Program, 2015AA020922), and the Fundamental Research Funds for the Central Universities (2017FZA7016). We appreciate C. B. Naman for critical editing of the manuscript.

ASSOCIATED CONTENT

Supporting Information.

The Supporting Information is available free of charge on the ACS Publications website at DOI:

Detailed synthetic procedures, supplementary figures, quantificaiton of Topoisomerase I inhibitory activity and NMR spectra

REFERENCES

(1) Nemes, A. (2010) Monoterpenoid indole alkaloids, CNS and anticancer drugs. In *Analogue-Based Drug Discovery II* (Fischer, J., Ganellin, C. R., Ed.), pp 189–215, John Wiley & Sons.

(2) Leonard, J. (1999) Recent progress in the chemistry of monoterpenoid indole alkaloids derived from secologanin. *Nat. Prod. Rep. 16*, 319–338.

(3) Stöckigt, J., Antonchick, A. P., Wu, F., Waldmann, H. (2011) The Pictet–Spengler reaction in nature and in organic chemistry. *Angew. Chem. Int. Ed. 50*, 8538–8564.

(4) Stöckigt, J., Panjikar, S. (2007) Structural biology in plant natural product biosynthesis–architecture of enzymes from monoterpenoid indole and tropane alkaloid biosynthesis. *Nat. Prod. Rep. 24*, 1382–1400.

(5) Stöckigt, J., Barleben, L., Panjikar, S., Loris, E. A. (2008) 3D-Structure and function of strictosidine synthase–the key enzyme of monoterpenoid indole alkaloid biosynthesis. *Plant Physiol. Biochem. 46*, 340–355.

(6) Wu, F., Zhu, H., Sun, L., Rajendran, C., Wang, M., Ren, X., Panjikar, S., Cherkasov, A., Zou, H., Stöckigt, J. (2012) Scaffold tailoring by a newly detected Pictet−Spenglerase activity of strictosidine synthase: from the common tryptoline skeleton to the rare piperazino-indole framework. *J. Am. Chem. Soc. 134*, 1498−1500.

(7) Pfitzner, U., Zenk, M. H. (1982) Immobilization of strictosidine synthase from Catharanthus cell cultures and preparative synthesis of strictosidine. *Planta Med. 46*, 10−14.

(8) Loris, E. A., Panjikar, S., Ruppert, M., Barleben, L., Unger, M., Schübel, H., Stöckigt, J. (2007) Structure-based engineering of strictosidine synthase: auxiliary for alkaloid libraries. *Chem. Biol. 14*, 979–985.

(9) Maresh, J. J., Giddings, L. A., Friedrich, A., Loris, E. A., Panjikar, S., Trout, B. L., Stöckigt, J., Peters, B., O'Connor, S. E. (2008) Strictosidine synthase: mechanism of a Pictet−Spengler catalyzing enzyme. *J. Am. Chem. Soc. 130*, 710–723.

(10) Yang, L., Zou, H., Zhu, H., Ruppert, M., Gong, J., Stöckigt, J. (2010) Improved expression of His(6)-tagged strictosidine synthase cDNA for chemo-enzymatic alkaloid diversification. *Chem. Biodivers. 7*, 860–870.

(11) Zhu, H., Kerčmar, P., Wu, F., Rajendran, C., Sun, L., Wang, M., Stöckigt, J. (2015) Using strictosidine synthase to prepare novel alkaloids. *Curr. Med. Chem. 22*, 1880–1888.

(12) Zou, H., Zhu, H., Zhang, L., Yang, L., Yu, Y., Stöckigt, J. (2010) A facile chemoenzymatic approach: one-step syntheses of monoterpenoid indole alkaloids. *Chem. Asian J. 5*, 2400–2404.

(13) Wall, M. E., Wani, M. C., Cook, C. E., Palmer, K. H., McPhail, A. T., Sim, G. A. (1966) The isolation and structure of camptothecin, a novel alkaloidal leukemia and tumor inhibitor from *Camptotheca acuminata*. *J. Am. Chem. Soc. 88*, 3888–3890.

(14) Capranico G., Marinello J., Chillemi G. (2017) Type I DNA topoisomerases. *J. Med. Chem. 60*, 2169−2192.

(15) Martino, E., Volpe, S. D., Terribile, E., Benetti, E., Sakaj, M., Centamore, A., Sala, A., Collina, S. (2017) The long story of camptothecin: from traditional medicine to drugs. *Bioorg. Med. Chem. Lett. 27*, 701–707.

(16) Pommier, Y. (2009) DNA topoisomerase I inhibitors: chemistry, biology, and interfacial inhibition. *Chem. Rev. 109*, 2894–2902.

(17) Park, Y. H., Chung, C. U., Park, B. M., Park, M. R., Park, D. I., Park, H. S., Kim, J. W., Jung, S. S., Kim, J. O., Kim, S. Y., Lee, J. E. (2016) Lesser toxicities of belotecan in patients with small cell lung cancer: a retrospective single-center study of camptothecin analogs. *Can. Respir. J. 2016*, 1–8.

(18) Gokduman K. (2016) Strategies targeting DNA topoisomerase I in cancer chemotherapy: camptothecins, nanocarriers for camptothecins, organic non-camptothecin compounds and metal complexes. *Curr. Drug Targets 17*, 1928–1939.

(19) Sheng, C., Miao, Z., Zhang, W. (2011) New strategies in the discovery of novel non-camptothecin topoisomerase I inhibitors. *Curr. Med. Chem. 18*, 4389–4409.

(20) Cragg, G. M., Newman, D. J. (2004) A tale of two tumor targets: topoisomerase I and tubulin. The Wall and Wani contribution to cancer chemotherapy. *J. Nat. Prod. 67*, 232–244.

(21) Han, B., Stockwin, L. H., Hancock, C., Yu, S. X., Hollingshead, M. G., Newton, D. L. (2010) Proteomic analysis of nuclei isolated from cancer cell lines treated with indenoisoquinoline NSC 724998, a novel topoisomerase I inhibitor. *J. Proteome Res. 9*, 4016–4027.

(22) Kurtzberg, L. S., Roth S., Krumbholz, R., Crawford, J., Bormann, C., Dunham, S., Yao, M., Rouleau, C., Bagley, R. G., Yu, X. J., Wang, F., Schmid, S. M., Lavoie, E. J., Teicher, B. A. (2011) Genz-644282, a novel non-camptothecin topoisomerase I inhibitor for cancer treatment. *Clin. Cancer Res. 17*, 2777-2787.

(23) Dong, G., Sheng, C., Wang, S., Miao, Z., Yao, J., Zhang, W. (2010) Selection of evodiamine as a novel topoisomerase I inhibitor by structure-based virtual screening and hit optimization of evodiamine derivatives as antitumor agents. *J. Med. Chem. 53*, 7521−7531.

(24) Erdelmeier, C. A., Regenass, U., Rali, T., Sticher, O. (1992) Indole alkaloids with in vitro antiproliferative activity from the ammoniacal extract of *Nauclea orientalis*. *Planta Med. 58*, 43−48.

(25) Chen, D., Ma, G., He, M., Liu, Y., Wang, X., Yang, X. (2016) Anti–inflammatory activity of two new indole alkaloids from the stems of *Nauclea officinalis*. *Helv. Chim. Acta. 99*, 742−746.

(26) Au, T. Y., Cheung, H. T. (1973) New corynanthé alkaloids from *Strychnos angustiflora*. *J. Chem. Soc. Perkin Trans. 1*, 13−16.

(27) Berger, M. A., Felzenbaum, A., Fraenkel, A. (1987) A new route to the indolopyridonaphthyridine ring system: synthesis of *N*-benzyl-13b,14-dihydronauclefine and *N*-benzyl-13b,14-dihydroangustine. *Tetrahedron 43*, 5761−5768.

(28) Repke, D. B., Clark, R. D., MacLean, D. B. (1988) Synthesis of naucléfine, angustidine, angustine, and (±)-13b,14-dihydroangustine. *J. Chem. Soc. Chem. Comm. 6*, 439−440.

(29) Repke, D. B., Clark, R. D., Nelson, J. T., Maclean, D. B. (1989) Synthesis of naucléfine, angustidine, angustine, (±)-13b,14-dihydro-angustine and naulafine. *Tetrahedron 45*, 2541–2550.

(30) Brown, R. T., Charalambides, A. A. (1973) Synthesis of dihydroangustine. *Tetrahedron Lett. 49*, 4837–4838.

(31) Patthy-Lukats, A., Kocsis, A., Szabo, L. F., Podanyi, B. (1999) Configurative correlation and conformational analysis of strictosidine and vincoside derivatives. *J. Nat. Prod. 62*, 1492–1499.

(32) Sastry, G. M., Adzhigirey, M., Day, T., Annabhimoju, R., Sherman, W. (2013) Protein and ligand preparation: parameters, protocols, and influence on virtual screening enrichments. *J. Comput. Aid. Mol. Des. 27*, 221–234.

(33) Friesner, R. A., Murphy, R. B., Repasky, M. P., Frye, L. L., Greenwood, J. R., Halgren,T. A., Sanschagrin, P. C., Mainz, D. T. (2006) Extra precision glide: docking and scoring incorporating a model of hydrophobic enclosure for protein-ligand complexes. *J. Med. Chem. 49*, 6177–6196.

(34) Halgren, T. A., Murphy, R. B., Friesner, R. A., Beard, H. S., Frye, L. L., Pollard, W. T., Banks, J. L. (2004) Glide: a new approach for rapid, accurate docking and scoring. 2. Enrichment factors in database screening. *J. Med. Chem. 47*, 1750–1759.

(35) Friesner, R. A., Banks, J. L., Murphy, R. B., Halgren, T. A., Klicic, J. J., Mainz, D. T., Repasky, M. P., Knoll, E. H., Shaw, D. E., Shelley, M., Perry, J. K., Francis, P., Shenkin, P. S. (2004) Glide: a new approach for rapid, accurate docking and scoring. 1. Method and assessment of docking accuracy. *J. Med. Chem. 47*, 1739–1749.

(36) Shivakumar, D., Williams, J., Wu, Y., Damm, W., Shelley, J., Sherman, W. (2010) Prediction of absolute solvation free energies using molecular dynamics free energy perturbation and the OPLS force field. *J. Chem. Theory Comput. 6*, 1509–1519.

(37) Guo, Z., Mohanty, U., Noehre, J., Sawyer, T. K., Sherman, W., Krilov, G. (2010) Probing the α-helical structural stability of stapled p53 peptides: molecular dynamics simulations and analysis. *Chem. Biol. Drug Des. 75*, 348-359.

(38) Valley, C. C., Cembran, A., Perlmutter, J. D., Lewis, A. K., Labello, N. P., Gao J., Sachs, J. N. (2012) The methionine-aromatic motif plays a unique role in stabilizing protein structure. *J. Biol. Chem. 287*, 34979−34991.